Association of Allelic Imbalance at Locus *D13S171* (*BRCA2*) and *p53* Alterations with Tumor Kinetics and Chromosomal Instability (Aneuploidy) in Nonsmall Cell Lung Carcinoma

V. G. Gorgoulis, M.D., Ph.D.[1,2]
A. Kotsinas, Ph.D.[1]
P. Zacharatos, Ph.D.[1,2]
G. Mariatos, B.Sc.[1]
T. Liloglou, Ph.D.[2]
E. Tsoli, M.Phil.[1]
S. Kokotas, B.Sc.[1]
C. Fassoulas, M.D.
J. K. Field, M.D., Ph.D.[2]
Ch. Kittas, M.D., Ph.D. [1]

[1] Department of Histology and Embryology, Medical School, University of Athens, Greece.

[2] Molecular Oncology Unit, Roy Castle International Centre for Lung Cancer Research, University of Liverpool, United Kingdom.

Supported by the National Greek Health Committee Grant A2α/6235/30-12-98 and the Program for Focussed Scholarships Grant 97YPER218.

P. Zacharatos, Ph.D., is a fellowship recipient of the Research Program for Focussed Scholarships (YPER97).

V. G. Gorgoulis, M.D., Ph.D., and A. Kotsinas, Ph.D. contributed equally.

Address for reprints: V. G. Gorgoulis, M.D., Ph.D., 53 Antaiou Street, Lamprini Ano Patissia, Athens, Greece GR-11146; Fax: 30-1-2928349; E-mail: histoclub@ axth.forthnet.gr

Received February 4, 2000; revision received June 16, 2000; accepted July 19, 2000.

BACKGROUND. *BRCA2* gene, located at chromosome 13q12.3, frequently is altered in familial types of cancer in which a "double-hit" inactivation model seems to occur. In contrast, in sporadic forms of cancer there is frequent absence of a second event (point mutations) suggesting that allelic imbalance at the *BRCA2* locus may be associated with a "gene dosage effect" of BRCA2 function. Little is known about *BRCA2* allelic alterations in nonsmall cell lung carcinomas (NSCLCs). Furthermore, recent studies suggest that BRCA2 and p53 participate in a common pathway involved in DNA damage repair. In view of this putative link, the authors investigated in a series of 63 NSCLCs: 1) the allelic imbalance (AIm) at the *D13S171* (*BRCA2*) locus, 2) the possible relation with tumor kinetics (proliferation [PI] and apoptotic indices [AI]) and chromosomal instability (aneuploidy) of the carcinomas, and 3) the mutual impact of *D13S171* AIm and p53 altered status on the above-mentioned parameters.

METHODS. Allelic status of the *BRCA2* region was examined in a series of 63 NSCLCs, by using the polymorphic marker *D13S171*, which is located in the center of it. Most information regarding the status of p53 at the immunohistochemical and genetic levels was obtained from a previous analysis. Tumor kinetic parameters (proliferation and apoptotic indices) were determined using Ki-67 immunohistochemical analysis and Tdt-mediated dUTP nick end labeling assay, respectively. Chromosomal instability (aneuploidy) was assessed by measuring nuclear DNA ploidy with an image analysis system.

RESULTS. Allelic imbalance at *D13S171*(*BRCA2*) was observed in 70% of the informative cases (H: heterozygous) with a rather high frequency of occurrence (50%) in Stage I disease, suggesting a possible early involvement in the development of NSCLCs. Although no association was found among loss of heterozygosity (LOH) at *D13S171*, kinetic parameters and ploidy status of the tumors and concurrent alterations in *BRCA2* and p53 (*BRCA2*[LOH]/p53[P]), which was the most frequent profile (37.2%), had the highest growth index (PI/AI mean value ratio) that differed significantly only from the *BRCA2*(LOH)/p53(N) pattern ($P = 0.027$). This difference was attributed to the high AI of the *BRCA2*(LOH)/p53(N) pattern ($P < 0.001$), whereas PI was similar among all *BRCA2*/p53 profiles. Also the "full abnormal pattern" was associated with aneuploidy, whereas the *BRCA2*(LOH)/p53(N) profile was mainly diploid. When these indicators and conventional prognostic ones were examined for effect on patient survival, only stage and lymph node status showed a significant correlation, whereas LOH at *D13S171* (*BRCA2*), p53 abnormalities, proliferative and apoptotic indices, ploidy status, smoking history, and histology and combinations of LOH and p53 abnormalities failed to show significant correlation with survival.

CONCLUSIONS. These findings suggest that in *BRCA2*(LOH) NSCLCs the status of p53 (wild type or mutant) represents a decisive determinant of tumor growth and chromosomal instability. Nevertheless, a possible synergistic effect from loss of *D13S171* region with p53 abnormalities cannot be excluded because the *BRCA2*(LOH)/p53(P) profile compared with the *BRCA2*(H)/p53(P) one had a higher PI/AI mean value ratio (31.05 vs. 22.97), although it was not statistically significant. However, we cannot exclude the possibility that LOH at *D13S171* reflects deletion of other putative tumor suppressor gene(s) in the proximity of BRCA2. In this respect, more studies are needed to understand the involvement of *BRCA2* region alterations in nonsmall cell lung carcinogenesis. ***Cancer* 2000;89:1933–45.**

KEYWORDS: proliferation index, apoptosis, aneuploidy, loss of heterozygosity (LOH), *BRCA2*, p53, *D13S171*.

A variety of genetic alterations have been observed in nonsmall cell lung carcinomas (NSCLCs), which include gains and/or losses of chromosomal regions.[1–3] In NSCLCs, the most frequently involved chromosome regions are 1q, 2q, 3p, 5q, 8q, 9p, 13q, and 17p.[1,4–7] One of these sites of great interest is the chromosomal arm 13q. In this area, several important tumor suppressor genes (TSGs), like *Rb1* (retinoblastoma) and *BRCA2*, are located.

BRCA2 is a large gene consisting of 27 exons. It covers a region of approximately 80 kilobases (kb) coding for a predicted protein of 3418 amino acids (384 kilodaltons) and is located at 13q12.3 (reviewed in Brody and Biesecker[8]). The gene encodes a nuclear protein that is cell cycle regulated and is mainly induced during the G1- to S-phase transition.[9–12] *BRCA2* is widely transcribed at low levels but appears to be highly expressed in rapidly proliferating cells.[9–12] In the cell, BRCA2 is involved in the maintenance of genome integrity,[13,14] although its precise function is not clear yet. Although it bears little homology with BRCA1, they both colocalize along with RAD51 in the nucleus in response to DNA damage.[11]

Mutations of *BRCA2* confer a high lifetime risk of female breast and ovarian carcinoma and are associated with an increased risk of male breast, prostate, and pancreatic carcinoma, and to a lesser extent with lung, bladder, and renal carcinoma and melanoma.[15] Reports until now show that, as far as hereditary forms of cancer are concerned, *BRCA2* behaves as a classic TSG, in which inactivation of both alleles is required for initiation of malignancy.[8,14,16,17] Germ line mutations are complemented by loss of heterozygosity (LOH) in the remaining allele, initiating the process for tumor development.[8,16,17]

However, in sporadic forms the situation is different, even controversial. Mutations in *BRCA2* are very rare[18] and can occur throughout the gene, with most of them predicted to result in a truncated protein.[8,16,17] The most frequent type of genetic alteration ascribed to the 13q12.3 area is allelic imbalance.[8,15–17] Loss of heterozygosity in the *BRCA2* region has been observed in breast, ovarian, and other types of sporadic carcinomas .[8] Allelic losses at *BRCA2* are associated with various clinicopathologic features.[19–21] These findings suggest that a reduction in *BRCA2* gene dosage to hemizygosity may be associated with neoplasia and there is not necessarily a need for a second allele loss.[22] Similar situations have been reported for *BRCA1*[23–25] and *p53*.[26]

p53 protein is a vital G1 to S and G2 to M factor that monitors DNA damage, as well as other stress signals inducing either cell cycle arrest or apoptosis.[27] Alterations of *p53* are considered the most common genetic lesion in human malignancies[28] including NSCLCs.[1] Recent lines of evidence show that *p53* is activated in a downstream fashion in response to failure of the BRCA2-dependent DNA repair mechanism (reviewed in Brugarolas and Jacks[29]). Particularly, in *BRCA2*-deficient tumors, loss of the p53 checkpoint is required for tumor progression.[30] In addition, Patel et al. observed in *BRCA2* truncated mouse embryo fibroblasts (MEFs) elevated p53 expression leading to proliferation impediment (G1 and G2/M arrest).[31] In a later study, MEFs deficient in *BRCA2* were accompanied by macroscopic chromosomal abnormalities.[31] These alterations arise from malfunctions in the repair process of double-strand breaks and chromosome recombination mechanisms, which in turn involve RAD51 as a basic component.[13] Notably, RAD51 apart from forming a complex with BRCA2, also interacts directly with p53 in response to chromosomal instability.[32]

In view of the apparent link between BRCA2 and p53, we investigated in a previously examined series of NSCLCs[33] the following: 1) the status of the *BRCA2* region, using the polymorphic marker *D13S171* located at the center of the aforementioned chromo-

somal area (Fig. 1),[34,35] 2) the possible relation among allelic imbalance (AIm) at the *BRCA2* region, kinetic parameters (proliferative activity and apoptotic index), and chromosomal instability (aneuploidy), which represents one of the forms of "genetic instability,"[36] of the tumors, and 3) the association of *BRCA2* AIm with altered p53 status and their mutual impact on the above parameters. To our knowledge, this information in NSCLCs has not been addressed so far.

MATERIALS AND METHODS

Tissue Samples

Sixty-three NSCLCs and adjacent normal lung tissue were analyzed. These tumors were part of a panel of 68 NSCLCs previously investigated for a G1-phase protein network including p53[33] (Table 1).

Microdissection and DNA Extraction

Microdissection

For DNA extraction, contiguous 5-μm sections were microdissected as previously described.[33]

DNA extraction

DNA was extracted from 50 μg of neoplastic material by using the phenol/chloroform/isoamylalcohol method.[38]

AIm Analysis of Microsatellite Loci *D13S171* and *D17S2179E*

We chose two markers to examine allelic alterations of *BRCA2* and *p53*, respectively: *D13S171*, which was selected from the Linkage Mapping Set v2.0 (PE-Applied Biosystems, Warrington, UK) and lies in the *BRCA2* region (Fig. 1), and *D17S2179E*, a pentanucleotide marker located within the first intron of *p53* (GenBank accession number U458658).

Method

The markers were amplified in a panel of duplex reactions. The reaction mixture consisted of: 1 $\times$ GeneAmp buffer II, 250 μM dNTPs, 2 mM $MgCl_2$, and 2 U AmpliTaq Gold polymerase. The polymerase chain reaction amplification parameters were initial denaturation for 12 minutes at 95 °C, 30 cycles of 30 seconds at 94 °C, 30 seconds at 55 °C, and 30 seconds at 72 °C, followed by a final extension of 20 minutes at 72 °C (Thermal Cycler 9700; PE-Applied Biosystems). The products were denatured in loading buffer (size marker ROX-350/dextran blue/formamide: 1/1/5) at 95 °C for 5 minutes and analyzed on an ABI-PRISM 377 Automatic Sequencer (PE-Applied Biosystems). Results were evaluated using the Genescan and Genotyper software (PE-Applied Biosystems).

Evaluation

To avoid within reaction variability and consequently to confirm the reproducibility of the assay, cutoff values were set as previously described.[39] When the allele ratio values were less than or equal to 0.65 or greater than or equal to 1.54, samples were scored as LOH, whereas, when their values covered the range 0.77–1.23, they were scored negative. Samples showing values 1.23–1.54 or 0.65–0.77 were subjected to a second assay and scored as LOH only if a second positive value was obtained.

Immunohistochemistry (IHC) of Ki-67

Antibodies

For immunohistochemical analysis of Ki-67 nuclear antigen the following antibody (Abs) was used: MIB-1 (Class: IgG1, mouse monoclonal, epitope: Ki-67 nuclear antigen) (Oncogene Science Biodynamics, Athens, Greece).

Method

Immunohistochemistry was performed according to indirect streptavidin-biotin-peroxidase method, as previously described.[33]

Evaluation

Tumor cells were evaluated as positive when nuclear staining, without cytoplasmic background, was observed. Proliferative index (PI) was estimated as the percentage of MIB-1 positive cells in 10 high-power fields (HPFs) (counted cells, > 1000). Slide examination was performed by three independent observers (V.G.G., P.Z., and C.K.). Intraobserver variability was minimal ($P < 0.01$).

IHC of p53

p53 immunohistochemical status was obtained from our previous work.[33] Tumors were considered p53 positive (P) when greater than 20% of the tumor cells show nuclear staining. The remaining tumors were scored as negative (N).[33]

p53 Gene Analysis

In this study, additional mutation analysis by single-strand conformation polymorphism and automated sequencing[33] was performed in samples 62 (exon 8, codon 270: TTT→ ATT, amino acid substitution: F→F), 44 (exon 6, codon 213: CGA→GA, frameshift mutation), and 27 (exon 8, codon 282: CGG→GG, frameshift mutation), which were not examined in our previous study.[33]

TABLE 1
Summary of Clinicopathologic Features, p53, D13S171 and D13S153 Status, Kinetic Parameters, and Ploidy Status

Sample	Smoking[a]	*D13S171* AIm	*D13S153* AIm[b]	p53 status IHC[b]	PI (%)	AI (%)	Ploidy	Histology
40	Yes	H	—	N	31	NE	A	UL
44	No	H	H	N	22.3	0.7	A	AD
46	No	H	H	N	NE	NE	D	AD
51	Yes	H	H	N	20.0	2.9	D	AD
4	Yes	H	H	P	NE	NE	A	UL
15	Yes	H	LOH	P	40.6	1.1	A	SQ
17	Yes	H	H	P	27.3	1.2	NE	SQ
18	Yes	H	H	P	43.6	4.8	D	SQ
38	Yes	H	—	P	39.3	3	A	SQ
52	Yes	H	LOH	P	39.0	0.6	A	SQ
53	Yes	H	LOH	P	51.2	2.6	A	SQ
61	Yes	H	LOH	P	24.5	1.1	D	AD
65	Yes	H	Ho	P	70.4	0.7	A	SQ
21	Yes	LOH	H	N	34.5	NE	D	SQ
23	Yes	LOH	LOH	N	26.7	2.6	D	AD
27	No	LOH	LOH	N	13.3	3.5	NE	AD
31	Yes	LOH	LOH	N	21.2	3	D	AD
34	Yes	LOH	—	N	34.7	0.5	D	AD
36	No	LOH	—	N	28.8	NE	A	AD
37	No	LOH	LOH	N	28.9	3.2	A	AD
39	Yes	LOH	H	N	54.0	0.9	D	SQ
45	Yes	LOH	Ho	N	32.9	8.9	D	AD
50	No	LOH	Ho	N	18.1	1.4	D	AD
54	Yes	LOH	LOH	N	32.2	3.1	NE	SQ
62	Yes	LOH	Ho	N	41.4	1.4	A	SQ
2	Yes	LOH	LOH	NE	NE	NE	NE	SQ
7	Yes	LOH	LOH	P	27.2	1.2	A	SQ
9	Yes	LOH	LOH	P	30.3	2	D	AD
10	Yes	LOH	LOH	P	40.6	1.8	A	UL
11	Yes	LOH	LOH	P	36.0	0.7	A	SQ
16	Yes	LOH	H	P	4.6	0.8	D	AD
24	Yes	LOH	Ho	P	26.7	0.8	NE	SQ
28	Yes	LOH	LOH	P	40.9	1.5	A	SQ
29	Yes	LOH	Ho	P	43.4	2.7	A	UL
35	Yes	LOH	—	P	29.2	0.8	A	AD
42	Yes	LOH	LOH	P	43.8	0.6	A	SQ
47	Yes	LOH	LOH	P	54.4	0.5	A	SQ
58	No	LOH	LOH	P	46.0	0.6	A	AD
59	Yes	LOH	LOH	P	30.4	NE	A	AD
60	Yes	LOH	LOH	P	38.6	1	A	AD
67	No	LOH	H	P	20.2	0.6	D	AD
69	Yes	LOH	—	P	NE	0.9	A	AD
19	Yes	LOH	LOH	N	NE	10.6	D	AD
13	Yes	NI	H	P	32.8	NE	D	SQ
57	Yes	NI	H	P	40.0	1.8	A	SQ
20	Yes	Ho	LOH	N	24.6	3.5	D	SQ
25	No	Ho	H	N	21.3	1.4	D	AD
33	Yes	Ho	—	N	40.7	0.8	A	SQ
66	Yes	Ho	LOH	N	33.3	2.3	A	SQ
1	Yes	Ho	H	P	31.1	4.8	A	AD
14	Yes	Ho	LOH	P	38.5	1.3	A	SQ
55	No	Ho	Ho	P	43.3	0.8	A	AD
56	Yes	Ho	LOH	P	47.3	0.4	A	SQ
64	Yes	Ho	LOH	P	39.3	1.6	D	AD
3	Yes	—	—	N	28.3	1.6	A	SQ
22	Yes	—	—	N	46.6	1.5	D	AD
30	Yes	—	—	N	28.8	5.2	D	UL
43	No	—	—	N	21.4	3.5	A	AD
49	No	—	—	N	36.9	NE	D	AD
26	Yes	—	—	P	29.2	0.1	A	AD
48	Yes	—	—	P	44.0	0.5	D	SQ
63	Yes	—	—	P	50.6	1	A	AD
68	Yes	—	—	P	59.1	2.1	A	SQ

AIm: allelic Imbalance analysis; IHC: immunohistochemistry; PI: proliferation index; AI: apoptotic index; H: heterozygous; N: negative; NE: not evaluable; A: aneuploid; UL: undifferentiated large cell carcinoma; AD: adenocarcinoma; D: diploid; LOH: loss of heterozygosity; P: positive; SQ: squamous cell carcinoma; Ho: homozygous; NI: not informative.

[a] All patients were current smokers.

[b] Data obtained from previous work.[33,38]

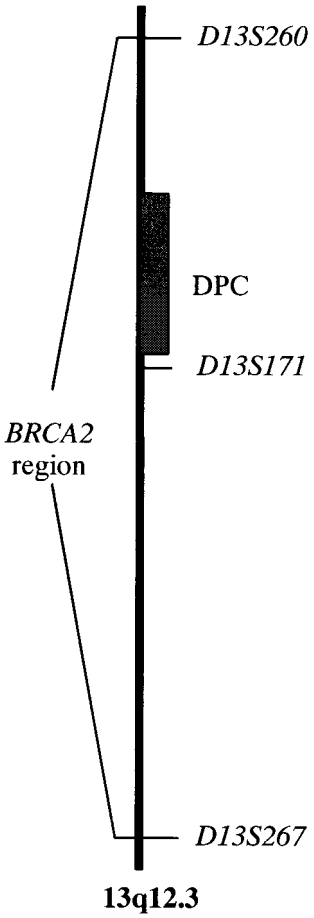

FIGURE 1. Map of the chromosomal area 13q12.3 representing the *BRCA2* region. The 2–3-cM subchromosomal fragment also includes the deleted in pancreatic carcinoma (DPC) fragment.[32]

Tdt-Mediated dUTP Nick End Labeling Assay (TUNEL)

Method

Double-strand DNA breaks were detected by TUNEL.[40] Briefly, 5-μm paraffin sections of the lesions were mounted on poly-L-lysine coated slides, dewaxed, rehydrated, and incubated for 30 minutes with 0.3% hydrogen peroxide to quench the endogenous peroxidase activity. Pretreatment was performed by incubating the sections with Proteinase K (Sigma, Athens, Greece) (20 μg/mL) for 15 minutes at 37 °C. The labeling step was performed with TdT (15 U per slide; New England Biolabs, Bioline, Athens, Greece) for 1 hour at 37 °C in 25 mM Tris-Cl, pH 7.2, 200 mM potassium cacodylate, 0.25 mM $CoCl_2$, 250 mg/mL bovine serum albumin, 24 μM biotin-dATP (Life Technologies, AntiSel, Athens, Greece). Reaction was stopped by rinsing the sections in 20 mM ethylenediamine tetraacetic acid. Next stage comprised a 30-minute incubation in StreptAB Complex solution (1:100 stock biotin solution, 1:100 stock streptavidin-peroxidase solution; Dako, Kalifronas, Athens, Greece). For color development we used 3,3′-diaminobenzidine tetrahydrochloride (DAB) as chromogen and hematoxylin as counterstain.

Controls

We used as positive controls tissue sections incubated with DNAse I before treatment with TdT and as negative ones sections incubated in TdT buffer without the presence of the enzyme.

Evaluation

Cells were considered to undergo apoptosis when nuclear staining, without cytoplasmic background, was observed. Apoptotic index was estimated as the percentage of apoptotic cells in 10 HPFs (counted cells, 900–10,000). Slide examination was performed by three independent observers (V.G.G., P.Z., and C.K.). Intraobserver variability was minimal ($P < 0.01$).

Nuclear DNA Ploidy Analysis

Method

The samples were stained according to the Thionin–Feulgen procedure.[41] Briefly, 5-μm paraffin sections were dewaxed, rehydrated in descending alcoholic solutions, and subjected to acidic hydrolysis in 5 N HCl at room temperature (RT) for 1 hour. The sections were stained with Thionin–Schiff reagent (0.5% thionin, 0.5% sodium bisulfide, 0.1 normal HCl) for 90 minutes at RT. Next, specimens were washed 3 times (30 seconds, 5 minutes, and 10 minutes) in freshly prepared sulfide solution (0.5% sodium bisulfide, 0.05 N HCl) and rinsed under running tap water for 10 minutes. An additional rinsing step in acidic alcohol (70% alcohol, 0.1 normal HCl) was used to increase the staining contrast. Finally, the sections were dehydrated in an ascending alcoholic scale and mounted in a xylene-based material.

Evaluation

The measuring procedure was performed using the Optipath TV-based image analysis system (Meyer Instruments, Houston, TX) equipped with a microscope and a video charge-coupled device camera. As internal reference, control lymphocytes or granulocytes were used. In each analysis, approximately 100 control and 350 tumor cells were measured. To distinguish nondiploid cells from diploid, an upper limit of 2.5c was set for diploid values. Because the fraction above 2.5c might include proliferating diploid cells, we also calculated the fraction of tumor cells with DNA values above the 5c level, which exceeds those of proliferating diploid cells. Cases with greater than 5% of cells

with DNA content above 5c limit were considered as aneuploid.[42]

Statistical Analysis

The possible associations between *D13S171* and p53 status, independently, *D13S171*/p53 patterns with PI, log apoptosis (logAI), ploidy status, and clinicopathologic parameters were assessed with the nonparametric Pearson chi-square and Kruskal–Wallis tests (Table 2). Furthermore, analysis of variance (ANOVA) was used to evaluate more specifically the possible association between p53 IHC, *D13S171* AIm, *D13S171*/p53 patterns with PI and logAI, respectively (Table 3). Logistic regression model formulation was applied for estimating possible associations between p53 IHC, *D13S171* AIm, *D13S171*/p53 patterns and ploidy status (Table 3). Finally, the Kaplan–Meier methodology was used for assessing the survival curves of the parameters examined in the current study. Differences between survival curves were examined by the log rank test. Analysis was performed with the SAS statistical package. The statistical difference was considered significant, when the *P* value was less than 0.05.

RESULTS

D13S171 (*BRCA2*) Analysis

Loss of heterozygosity at *D13S171* (*BRCA2*) (*BRCA2*/[LOH]) was observed in 30 of 43 informative cases (70%) (Table 1 and Fig. 2). This marker resides centrally to the *BRCA2* region and has been used frequently for assessing allelic losses at this locus (Fig. 1).[19,20,34,35,43] No significant association was noticed between the histologic type, lymph node invasion, ploidy status, stage of the disease, and *BRCA2* status (Table 2).

p53 Analysis

IHC and relation with clinicopathologic parameters

Expression of p53 was observed in 36 of 62 informative cases (58.1%). The association of p53 with the clinicopathologic parameters of the patients is summarized in Table 2. A significant association was observed between p53 positive staining and smoking ($P = 0.015$ by Pearson chi-square [Table 2] and $P = 0.016$; odds ratio, 0.172 [0.041, 0.719] by logistic regression analysis).

p53 *gene alterations*

The additional sequence analysis in our database revealed 2 frameshift (Cases 44 and 27) and 1 silent (Case 62) *p53* mutations. A highly significant association was observed between *p53* gene mutations and p53 immunostaining (positive vs. negative; 20 of 36 vs. 5 of 26, $P = 0.002$ by Pearson chi-square). Allelic imbalance analysis with *D17S2179E* showed alter-

TABLE 2
Association between *D13S171*, p53, *D13S171*/p53 Patterns and Clinicopathologic Features, Proliferation Index, Apoptotic Index, and Ploidy Status

	Pearson chi-square test																Kruskal–Wallis test						
	Smoking history			Histology				Lymph node invasion			Stage				Ploidy status			Proliferation index			Apoptotic index			
Expression	Yes	No	*P* value	Sq	Ad	UL	*P* value	+	–	*P* value	I	II	III	*P* value	A	D	*P* value	Mean (n)	SD	*P* value	Mean (n)	SD	*P* value	PI/AI ratio[a]
D13S171																								
H	11	2	0.721	7	4	2	0.269	7	6	1.000	4	4	5	0.457	8	4	0.6	37.20 (11)	14.744	0.562	1.87 (10)	1.392	0.887	19.89
LOH	24	6		11	17	2		17	13		15	8	7		15	11		32.556 (27)	11.469		2.138 (26)	2.444		15.22
p53 IHC																								
N	17	9	0.02	8	16	2	0.549	12	14	0.441	15	7	4	0.106	9	15	0.006	30.079 (24)	9.475	0.004	2.976 (21)	2.565	0.002	10.1
P	33	3		19	14	3		21	15		12	11	13		26	8		38.335 (34)	12.006		1.394 (33)	1.12		27.5
D13S171/p53																								
H/N	2	2	0.088	0	3	1	0.046	2	2	0.915	2	1	1	0.740	2	2	0.031	24.433 (3)	1.66	0.067	1.8 (2)	1.556	0.033	13.57
LOH/N	9	4		4	9	0		8	5		6	4	3		3	8		30.558 (12)	11.77		3.555 (11)	3.247		8.6
H/P	10	0		8	1	1		6	4		2	4	4		7	2		43.889 (9)	15.41		1.911 (9)	1.372		22.97
LOH/P	14	2		6	8	2		8	8		9	4	3		12	3		34.153 (15)	12.53		1.1 (15)	0.634		31.05

Sq: squamous cell carcinoma; Ad: adenocarcinoma; UL: undifferentiated large cell carcinoma; A: aneuploid; D: diploid; SD: standard deviation; PI: proliferation index; AI: apoptotic index; H: heterozygous; LOH: loss of heterozygosity; N: normal; P: positive.

[a] PI/AI mean value ratio.

TABLE 3
Association between p53, *D13S171*/p53 Patterns and PI, AI, and Ploidy Status

	Analysis of variance						Logistic regression analysis	
	PI		log AI		PI/AI		Ploidy	
	Mean difference (95% CI)	*P* value	Mean difference (95% CI)	*P* value	Mean difference (95% CI)	*P* value	Odds ratio	*P* value
p53(P)	8.256 (2.362–14.151)	0.007	−1.582 (−2.6 to −0.564)	0.003	28.766 (3.632–53.9)	0.026	5.417 (1.724–17.020)	0.004
p53(N)	—		—		—		—	—
D13S171 (H)/p53(P)	9.720 (−11.622–31.062)	1.00	−0.700 (−4.870–3.470)	1.00	20.729 (−37.22–78.677)	1.00	0.250 (0.02–2.577)	0.244
D13S171 (LOH)/p53(N)	3.595 (−9.474–16.664)	1.00	−2.455 (−4.653 to −0.256)	0.022	18.509 (−13.231–50.248)	0.667	0.094 (0.015–0.57)	0.011
D13S171 (H)/p53(N)	−9.736 (−23.964–4.492)	0.383	−0.811 (−3.147–1.524)	1.00	4.840 (−27.912–37.592)	1.00	0.875 (0.116–6.58)	0.89
D13S171 (LOH)/p53(P)	—		—	—	—		—	—

PI: proliferation index; AI: apoptotic index; CI: confidence interval; P: positive; N: normal; H: heterozygous; LOH: loss of heterozygosity.

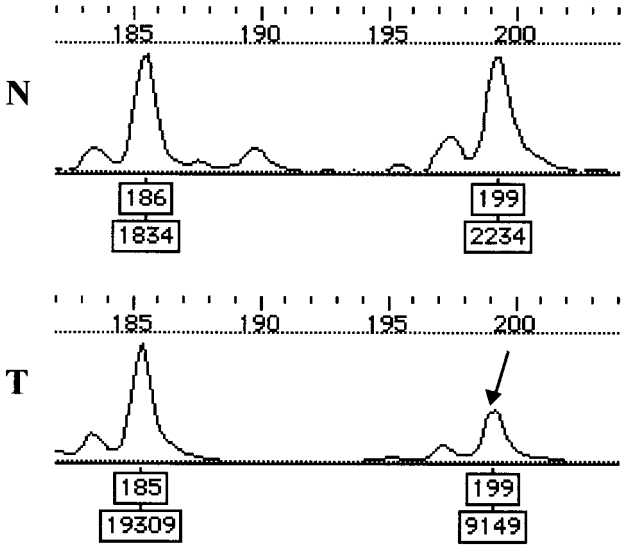

FIGURE 2. Representative result of allelic imbalance analysis (Case 10) with chromosome marker *D13S171* (see "Materials and Methods") N: normal sample; T: tumor sample. Loss of heterozygosity is indicated by an arrow.

ations in 14 of 21 informative samples (67%). Seven of these cases (50%) were accompanied with *p53* point mutations in the remaining allele.[33] Because the expression status of p53 is highly correlated with sequence analysis[33,37] and the number of informative specimens at the *D17S2179E* locus is rather low, we will consider in the following associations p53 immunohistochemical positivity (p53[P]) as an indicator of *p53* gene alterations.

Analysis of Tumor Kinetics (Proliferation and Apoptosis) and Ploidy Status. Relation with the *BRCA2*/p53 Patterns

Recent results on animal models have shown that p53 functions downstream of the BRCA complex repairing system.[30,31,44] Because of this apparent link, we investigated the *BRCA2*/p53 alteration profiles found in our series with the clinicopathologic features, kinetics and ploidy status of the tumors.

Tumor kinetics and ploidy status analysis

Proliferation index was assessed using MIB-1 (Ki-67), the most reliable antibody for estimating growth fraction by immunohistochemistry.[45] The percentages of cells positive for Ki-67 antigen, in the cancerous areas, ranged from 4.6% to 70.4%, with a mean value 34.9 ± 11.68 (58 evaluable cases; Table 1 and Fig. 3). Proliferation index was found increased in smoking subjects ($P = 0.015$ by Kruskal–Wallis) and in squamous cell carcinomas compared with adenocarcinoma ($P = 0.001$ by Kruskal–Wallis). The apoptotic index (AI) ranged from 0.1% to 10.6%, with a mean value 2.009 ± 1.961 (Table 1 and Fig. 4). No correlation between AI and clinicopathologic parameters of the patients was found. Ploidy analysis evaluated as aneuploid carcinomas 35 of the 58 informative cases (60.3%; Table 1 and Fig. 5). Aneuploid tumors had significantly higher PI ($P = 0.007$; mean difference (MD), 38.97 [35.22, 42.73] by ANOVA) and lower AI ($P = 0.02$; MD[logAI], 1.487 [1.091, 1.883] by ANOVA) than the diploid ones.

Relation with the BRCA2/p53 *patterns*

Correlation of *D13S171*(*BRCA2*) and p53 status independently, with tumor kinetics and ploidy showed that only the carcinomas with p53 alterations (p53[P]) were associated significantly with increased PI, decreased AI and aneuploidy compared with the p53(N) cases (Tables 2 and 3). Concurrent study of *BRCA2* and p53 status revealed all the theoretically expected patterns having the *BRCA2*(LOH)/p53(P) pattern the most frequent one (37.2%; Table 2). The PI among the various profiles did not have significant differences (Ta-

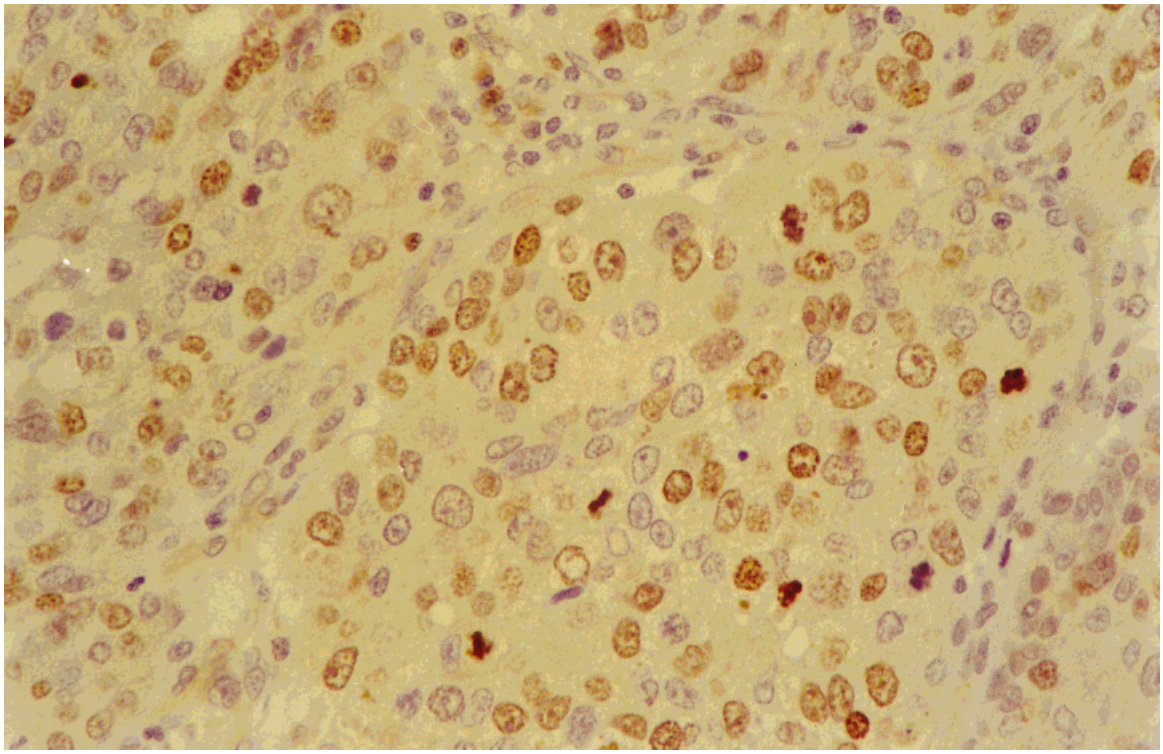

FIGURE 3. Squamous cell lung carcinoma (Case 18) with high proliferative activity (PI, 44%). Streptavidin-biotin-peroxidase technique (DAB as chromogen) with MIB-1 anti–Ki-67 antibody (see "Materials and Methods") and hematoxylin counterstain (original magnification ×400) were used.

ble 2). The *BRCA2*(LOH)/p53(P) pattern had the highest AI, that differed significantly only from the *BRCA2*(LOH)/p53(N) one ($P = 0.033$ by Kruskal–Wallis [Table 2] and $P = 0.022$ for logAI by ANOVA [Table 3]). The "full abnormal" pattern also had the highest PI/AI mean value ratio (31.05; Table 2 and Fig. 6). Furthermore, this profile was associated with aneuploidy more frequently than the *BRCA2*(LOH)/p53(N) pattern ($P = 0.031$ by Kruskal–Wallis [Table 2] and $P = 0.011$ by logistic regression analysis [Table 3]). No significant correlation between the four patterns and the clinicopathologic parameters of the patients was observed (Table 2).

Survival Analysis

Kaplan–Meier methodology was used to estimate the impact of each parameter examined in the current report on the patients survival status. During our study (follow-up duration up to 67 months), we have observed 34 failures and 26 censored cases. The median survival of the patients in our study was 25 months. Differences between survival curves were examined using the log rank test. Patients who have lymph node invasion show worse prognosis ($P < 0.001$; data not shown). Moreover, Stage I patients had better prognosis compared with Stages II and III.

DISCUSSION

In the current report, the status of *BRCA2* region was examined in NSCLCs, using the polymorphic marker *D13S171*, which is located at the center of this 2–3-cM region (Fig. 1) and has been frequently used as an indicator of alterations in this area.[19,20,34,35,43] Also, kinetic parameters (proliferative activity and apoptotic index) and chromosomal instability (aneuploidy) of the tumors were evaluated in relation to *BRCA2* allelic alterations, because the latter is involved in DNA repair mechanism.[13,14] In addition, the proposed functional link between BRCA2 and p53[14,29] led us to investigate their interrelation and the association between the observed patterns with the aforementioned parameters. To our knowledge, this is the first report dealing with this information.

Allelic imbalance at the *D13S171* locus was found at a high frequency 70% (30 of 43 informative cases). The rather high percentage of allelic loss in Stage I tumors (50%), suggests the relatively early involvement of this area in NSCL carcinogenesis. Similarly, a wide range of AIm at this region was found in other tumors such as breast,[21,46] ovarian,[47] prostate,[48,49] and esophageal ones.[43] AIm at *D13S171* most probably reflect alterations of the *BRCA2* gene for the following

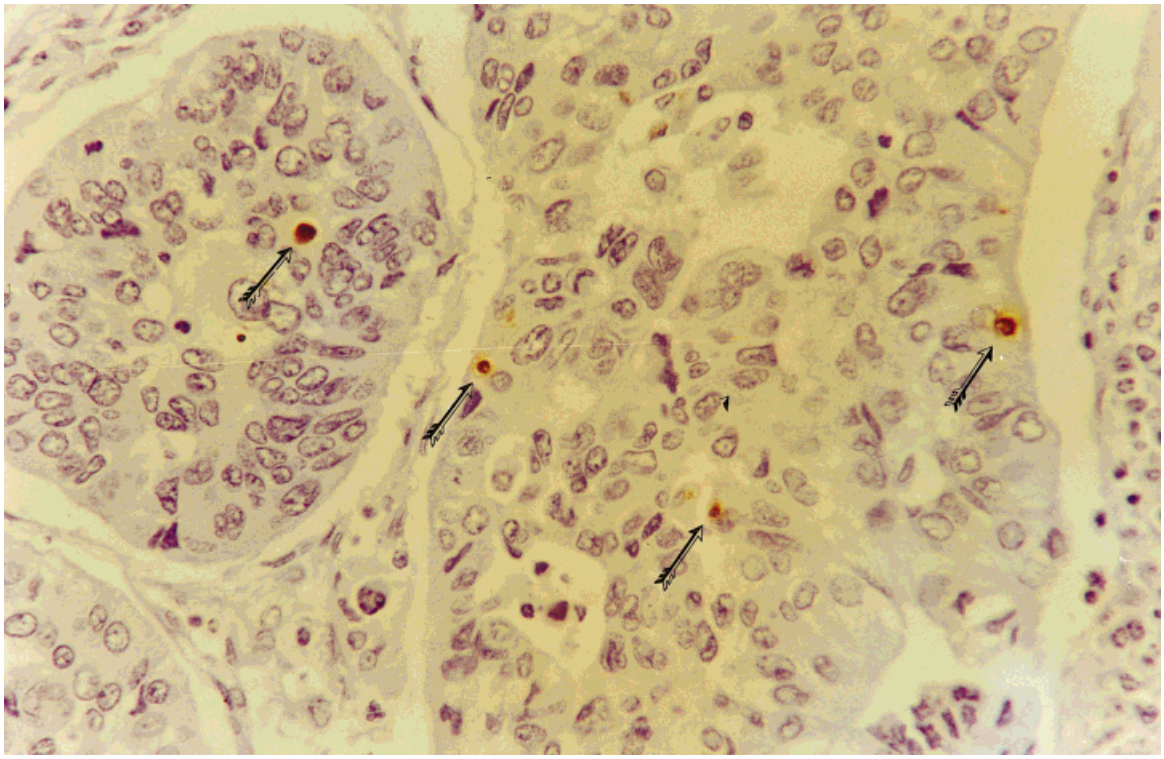

FIGURE 4. Lung adenocarcinoma (Case 64) with moderate apoptotic index (1.6%). Tdt-mediated dUTP nick end labeling assay (DAB as chromogen, see "Materials and Methods") and hematoxylin counterstain (original magnification ×400) were used.

reasons: 1) *BRCA2* is a large gene (80 kb) widespread in the above 2–3-cM area,[8,34] 2) the marker is located approximately in the center of this region (Fig. 1),[34,35] and 3) LOH at chromosome microsatellite markers usually involve large DNA segments (range from approximately 50 kb to the whole chromosome).[8] Although, TSGs usually are inactivated by two "hits," *BRCA2*, which has been characterized as such, shows a high frequency of allelic loss in sporadic tumors and a surprising lack of point mutations in the remaining allele.[8,18,22] Therefore, *BRCA2* may be involved in sporadic tumor carcinogenesis through a "gene dosage" effect, as suggested by Lancaster et al..[22] Such mechanisms have been shown for *BRCA1*[23–25] and *p53*.[26]

BRCA2 was shown to be involved in DNA damage response.[30,31] This function was attributed to a role in DNA damage repair via its interaction with RAD51,[13,14,17] a protein involved in the control of chromosome recombination and in the maintenance of genomic integrity.[13,14,17] Within this context, we investigated whether loss in the *BRCA2* region is associated with chromosomal instability (aneuploidy) of the tumors.[13,14,17] In our series, aneuploidy occurred at a high frequency (60.3%) but was not correlated with *D13S171* alterations. Similarly, *BRCA2* alterations were observed in tubular and lobular breast carcinomas, which are mainly diploid.[50,51] However, in mice blastocysts and MEFs, homozygous for truncations of *BRCA2* (*BRCA2*$^{TR/TR}$), numerous spontaneous chromosomal abnormalities have been reported.[31] Of note, these cells also had a severe impairment in proliferative activity, ending in cell cycle arrest.[30,44,52] This detrimental effect was partially rescued by wild-type (wt) p53 inactivation.[30,44] In these animal models, apoptosis was reported to be normal.[31,52]

These observations in animal models led us to investigate the relation between AIm at *D13S171* and the kinetic parameters of the tumors (AI and PI). Although, no significant associations were found when AIm at *BRCA2* was examined in combination with p53 expression, we noticed that concurrent alterations (*BRCA2*[LOH]/p53[P]), which was the most frequent pattern (37.2%), had a significantly higher growth index (PI/AI mean value ratio) from the group of carcinomas with the *BRCA2*(LOH)/p53(N) profile (Table 3). Of note, the different growth index between these two groups was due to the significantly higher AI observed in the *BRCA2*(LOH)/p53(N) tumors, whereas PI had similar values among all four *BRCA2*/p53 groups of carcinomas (Tables 2 and 3). In addition, the *BRCA2*(LOH)/p53(P) pattern was associated more frequently with aneuploidy, whereas the *BRCA2*(LOH)/

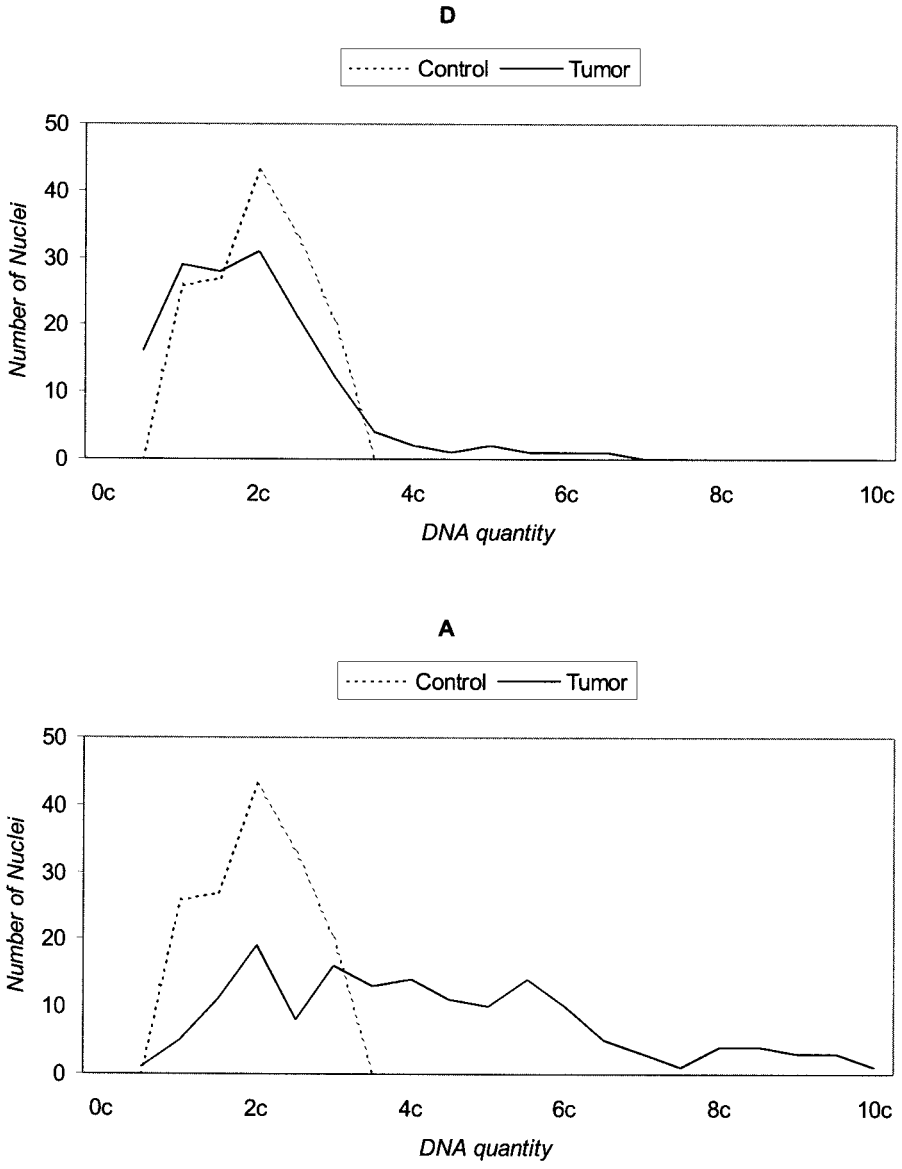

FIGURE 5. Diagrams present the DNA content of two representative tumors (ploidy analysis, see "Materials and Methods"). D: diploid tumor (Case 31); A: aneuploid tumor (Case 37).

p53(N) profile was mainly diploid (Tables 2 and 3). Thus, one can observe that the main determinant of the tumor growth index and ploidy status in the *BRCA2*(LOH) tumors, is the state of p53. Whenever p53 shows no alterations (wt p53), proliferation and apoptosis obtain the lowest and highest values, respectively, and tumors are mainly diploid (Tables 2 and 3). From these results, it is tempting to speculate that the proposed model by Brugarolas and Jacks, in which wt p53 leads to either growth arrest or apoptosis in *BRCA*-deficient cells,[29] may be valid in this group of NSCLCs. Similar wt p53 "protective" effects seem to exist with active oncogenes as well, such as *ras*,[53,54] *β-catenin*,[55] and c-*mos* (unpublished data).

Despite these findings and the apparent critical involvement of p53, the possible synergistic effect of *BRCA2* region allelic loss with altered p53 status cannot be ruled out, because the *BRCA2*(LOH)/p53(P) profile had a higher growth rate index than the *BRCA2*(H)/p53(P) one (31.05 vs. 22.97) although it was not statistically significant (Tables 2 and 3). Therefore, more studies are needed in larger series of tumor samples to draw final conclusions.

Another noteworthy point in BRCA-related tumors was raised by Crook et al. who showed in them the presence of novel *p53* mutations.[56] Specifically, these p53 mutants retain basic p53-dependent activities[56] but fail to suppress transformation and show gain of function transforming activities.[57] In the current report, we did not find these types of mutations, but more common ones,[28] which is in accordance with the results described by Crook et al., who showed

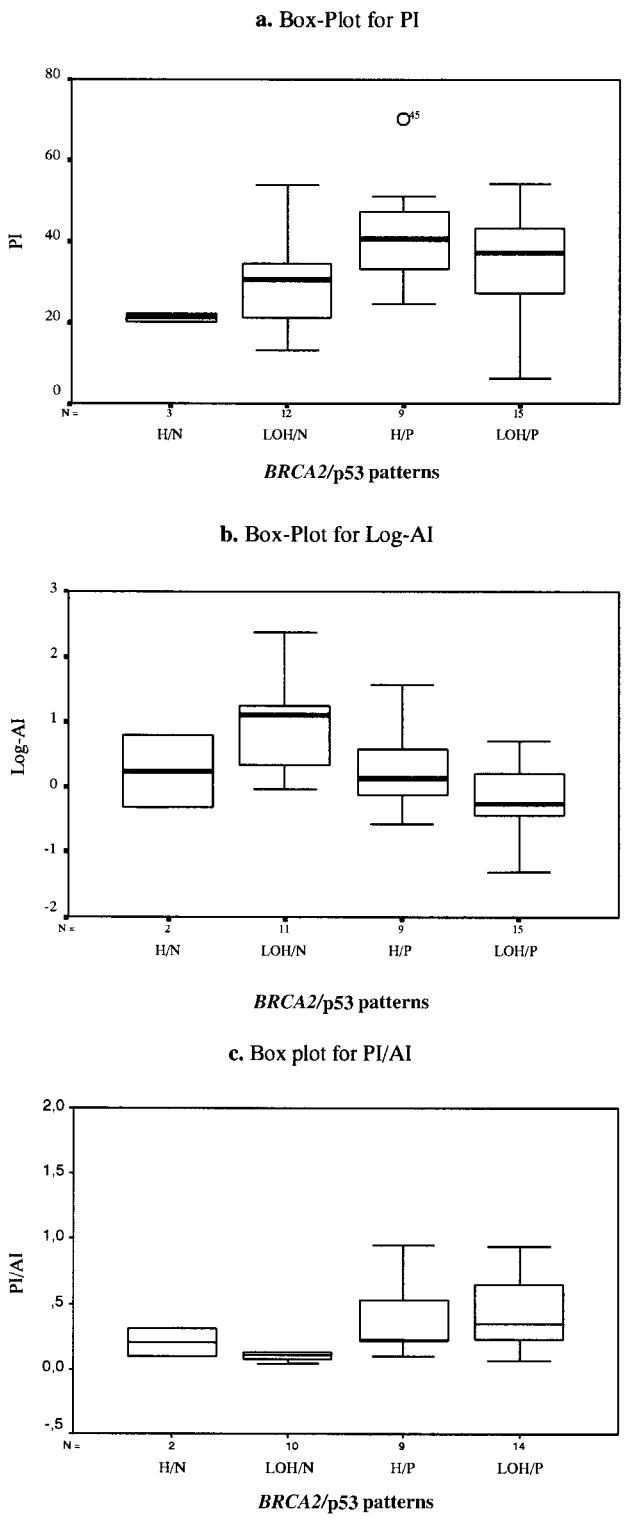

FIGURE 6. Box-plots present the proliferation index (PI) (a), apoptotic index (AI) (b), and PI/AI mean value ratios (c) of tumors with certain protein expression profiles. H: heterozygous; N: negative; P: positive; LOH: loss of heterozygosity.

that these novel p53 mutants were not present in BRCA-sporadic forms of breast carcinomas.[56] Nevertheless, we previously have reported that several of these common p53 mutants present in NSCLC environment also show gain of function activities,[58] able to discriminate between various p53 responsive elements of several cell cycle regulators.[59]

Also, note that the type of p53 point mutations detected in our samples belong to those commonly observed in typical lung carcinoma associated with smoking.[28] Notably, p53 overexpression also was associated with smoking ($P = 0.02$), reinforcing data derived from previous studies (reviewed in Sekido et al.[1]).

Alternatively, *D13S171* LOH could represent (co)deletion of other putative oncosuppressor gene(s) located in the vicinity of this marker.[35,43,48,49,60] Several reports have shown that allelic imbalance at *D13S171* does not necessarily reflect loss of *BRCA2* gene itself, but that of other genes in the proximity of this region.[48,49,61] Analysis at another marker, (*D13S153*) located at 13q14 area and within *RB1*, in our NSCLC subset showed a high frequency of allelic loss (65%) in this region (Table 1).[37] The concordance of LOH at both sites was also high (55%, $P = 0.04$ Pearson chi-square) suggesting a regional loss in the 13q12-14 area. In such a case, multiple gene deletions may have occurred in addition to *BRCA2*.

In summary, the current study demonstrated a high frequency of allelic imbalance at *D13S171* (*BRCA2*) locus in NSCLCs. These alterations are probably early events in NSCL carcinogenesis and frequently are associated with p53 alterations. Furthermore, the *BRCA2*(LOH)/p53(P) pattern seems to confer an additive effect on tumor growth, but further investigations are needed to confirm the implication of *BRCA2* alterations in lung carcinogenesis.

REFERENCES

1. Sekido Y, Fong KM, Minna JD. Progress in understanding the molecular pathogenesis of human lung cancer. *Biochim Biophys Acta* 1998;1378:F21–59.
2. Ullmann R, Schwendel A, Klemen H, Wolf G, Petersen I, Popper HH. Unbalanced chromosomal aberrations in neuroendocrine lung tumors as detected by comparative genomic hybridization. *Hum Pathol* 1998;29:1145–9.
3. Varella-Garcia M, Gemmill RM, Rabenhorst SH, Lotto A, Drabkin HA, Archer PA, et al. Chromosomal duplication accompanies allelic loss in non-small cell lung carcinoma. *Cancer Res* 1998;58:4701–7.
4. Shiseki M, Kohno T, Nishikawa R, Sameshima Y, Mizoguchi H, Yokota J. Frequent allelic losses on chromosomes 2q, 18q, and 22q in advanced non-small cell lung carcinoma. *Cancer Res* 1994;54:5643–8.
5. Fong KM, Zimmerman PV, Smith PJ. Tumor progression and loss of heterozygosity at 5q and 18q in non-small cell lung cancer. *Cancer Res* 1995;55:220–3.

6. Cooper CA, Bubb VJ, Smithson N, Carter RL, Gledhill S, Lamb D, et al. Loss of heterozygosity at 5q21 in non-small cell lung cancer: a frequent event but without evidence of apc mutation. *J Pathol* 1996;180:33–7.
7. Sanchez-Cespedes M, Rosell R, Pifarre A, Lopez-Cabrerizo MP, Barnadas A, Sanchez JJ, et al. Microsatellite alterations at 5q21, 11p13, and 11p15.5 do not predict survival in non-small cell lung cancer. *J Clin Cancer Res* 1997;3:1229–35.
8. Brody LC, Biesecker BB. Breast cancer susceptibility genes Brca1 and Brca2. *Medicine* 1998;77:208–6.
9. Vaughn JP, Cirisano FD, Huper G, Berchuck A, Futreal PA, Marks JR, et al. Cell cycle control of BRCA2. *Cancer Res* 1996,56:4590–4.
10. Rajan JV, Wang M, Marquis ST, Chodosh LA. Brca2 is coordinately regulated with Brca1 during proliferation and differentiation in mammary epithelial cells. *Proc Natl Acad Sci USA* 1996;93:13078–83.
11. Bertwistle D, Swift S, Marston NJ, Jackson LE, Crossland S, Crompton MR, et al. Nuclear location and cell cycle regulation of the BRCA2 protein. *Cancer Res* 1997;57:5485–8.
12. Wang SC, Lin SH, Su LK, Hung MC. Changes in BRCA2 expression during progression of cell cycle. *Biochem Biophys Res Commun* 1997;234:247–51.
13. Zhang H, Tombline G, Weber BL. BRCA1, BRCA2 and DNA damage response: collision or collusion? *Cell* 1998;92:433–6.
14. Gayther SA, Ponder BAJ. Clues to the function of the tumor susceptibility gene BRCA2. *Dis Markers* 1998;14:1–8.
15. Hesketh R. The oncogene and tumour suppressor gene facts book. 2nd ed. London: Academic Press, 1997.
16. Casey G. The BRCA1 and BRCA2 breast cancer genes. *Curr Opin Oncol* 1997;9:88–93.
17. Blackwood MA, Weber BL. BRCA1 and BRCA2: from molecular genetics to clinical medicine. *J Clin Oncol* 1998;16: 1969–77.
18. Teng DH, Bogden R, Mitchell J, Baumgard M, Bell R, Berry S, et al. Low incidence of BRCA2 mutations in breast carcinomas and other cancers. *Nat Genet* 1996;13:241–4.
19. Beckmann MW, Picard F, An HX, van Roeyen CR, Dominik SI, Mosny DS, et al. Clinical impact of detection of loss of heterozygosity of BRCA1 and BRCA2 markers in sporadic breast cancer. *Br J Cancer* 1996;73:1220–6.
20. Edwards SM, Dunsmuir WD, Gillett CE, Lakhani SR, Corbishley C, Young M, et al. Immunohistochemical expression of BRCA2 protein and allelic loss at the BRCA2 locus in prostate cancer. CRC/BPG UK familial prostate cancer study collaborators. *Int J Cancer* 1998;78:1–7.
21. Silva JM, Gonzalez R, Provencio M, Dominguez G, Garcia JM, Gallego I, et al. Loss of heterozygosity in BRCA1 and BRCA2 markers and high-grade malignancy in breast cancer. *Breast Cancer Res Treat* 1999;53:9–17.
22. Lancaster JM, Wooster R, Mangion J, Phelan CM, Cochran C, Gumbs C, et al. *BRCA2* mutations in primary breast and ovarian cancers. *Nat Genet* 1996;13:238–40.
23. Chen Y, Chen CF, Riley DJ, Allred DC, Chen PL, Von Hoff D, et al. Aberrant subcellular localization of BRCA1 in breast cancer. *Science* 1995;270:789–91.
24. Kainu T, Kononen J, Johansson O, Olsson H, Borg A, Isola J. Detection of germline BRCA1 mutations in breast cancer patients by quantitative messenger RNA in situ hybridization. *Cancer Res* 1996;56:2912–5.
25. Thompson ME, Jensen RA, Obermiller PS, Page DL, Holt JT. Decreased expression of BRCA1 accelerates growth and is often present during sporadic breast cancer progression. *Nat Genet* 1995;9:444–50.
26. Venkatachalam S, Shi YP, Jones SN, Vogel H, Bradley A, Pinkel D, et al. Retention of wild-type p53 tumors from p53 heterozygous mice: reduction of p53 dosage can promote cancer formation. *EMBO J* 1998;17:4657–67.
27. Prives C, Hall PA. The p53 pathway. *J Pathol* 1999;187:112–26.
28. Greenblatt MS, Bennett WP, Hollstein M, Harris CC. Mutations in the p53 tumor suppressor gene: clues to cancer etiology and molecular pathogenesis. *Cancer Res* 1995;54: 4855–78.
29. Brugarolas J, Jacks T. Double indemnity: p53, BRCA and cancer. *Nat Med* 1997;3:721–2.
30. Connor F, Bertwistle D, Mee PJ, Ross GM, Swift S, Grigorieva E, et al. Tumorigenesis and DNA repair defect in mice with a truncating Brca2 mutation. *Nat Genet* 1997;17:423–30.
31. Patel KJ, Vu VP, Lee H, Corcoran A, Thistlethwaite FC, Evans MJ, et al. Involvement of BRCA2 in DNA repair. *Mol Cell* 1998;1:347–57.
32. Sturzbecher HW, Donzelmann B, Henning W, Knippschild U, Buchhop S. p53 is linked directly to homologous recombination processes via RAD51/RecA protein interaction. *EMBO J* 1996;15:1992–2002.
33. Gorgoulis VG, Zacharatos P, Kotsinas A, Liloglou T, Kyroudi A, Veslemes M, et al. Alterations of the p16-pRb pathway and the chromosome locus 9p21-22 in non-small-cell lung carcinomas: relationship with p53 and MDM2 protein expression. *Am J Pathol* 1998;153:1749–65.
34. Grimmond SM, Palmer JM, Walters MK, Scott C, Nancarrow DJ, Teh BT, et al. Confirmation of susceptibility locus on chromosome 13 in Australian breast cancer families. *Hum Genet* 1996;98:80–5.
35. Schutte M, Rozenblum E, Moskaluk CA, Guan X, Hoque ATMS, Hahn S, et al. An integrated high-resolution physical map of the DPC/BRCA2 region at chromosome 13q12. *Cancer Res* 1995;55:4570–4.
36. Lengauer C, Kinzler KW, Vogelstein B. Genetic instabilities in human cancers. *Nature* 1998;396:643–9.
37. Gorgoulis VG, Zacharatos P, Kotsinas A, Mariatos G, Liloglou T, Vogiatzi T, et al. Altered expression of the cell cycle regulatory molecules pRb, p53 and MDM2 exert a synergistic effect on tumor growth and genomic instability in non-small cell lung carcinomas (NSCLCs). *Mol Med* 2000;6:208–37.
38. Davis LG, Dibner MD, Battey JF. Basic methods in molecular biology. New York: Elsevier Science, 1986.
39. Liloglou T, Maloney P, Xinarianos G, Fear S, Field JK. Sensitivity and limitations of high throughput fluorescent microsatellite analysis for the detection of allelic imbalance. Application in lung tumors. *Int J Oncol* 2000;16:5–14.
40. Gavrieli Y, Serman Y, Ben Sasson S. Identification of programmed cell death *in situ* via specific labeling of nuclear DNA fragmentation. *J Cell Biol* 1992;119:493–501.
41. Auer GU, Falkmer UG, Zetteberg AD. Image cytometric nuclear DNA analysis in clinical tumor material. In: Baak JPA, editor. Manual of quantitative pathology in cancer diagnosis and prognosis. Heidelberg: Springer, 1991:211–32.
42. Hirano T, Franzen B, Kato H, Ebihara Y, Auer G. Genesis of squamous cell lung carcinoma. Sequential changes of proliferation, DNA ploidy and p53 expression. *Am J Pathol* 1994;144:296–302.
43. Harada H, Tanaka H, Shimada Y, Shinoda M, Imamura M, Ishizaki K. Lymph node metastasis is associated with allelic loss on chromosome 13q12-13 in esophageal squamous cell carcinoma. *Cancer Res* 1999;59:3724–9.

44. Ludwig T, Chapman DL, Papaioannou VE, Efstratiadis A. Targeted mutations of breast cancer susceptibility gene homologs in mice: lethal phenotypes of BRCA1, BRCA2, BRCA1/BRCA2, BRCA1/p53 and BRCA2/p53 nullizygous embryos. *Genes Dev* 1997;11:1226–41.
45. Kawai T, Suzuki M, Kono S, Shinomiya N, Rokutanda M, Tagaki K, et al. Proliferating cell nuclear antigen Ki-67 in lung carcinoma: correlation with DNA flow cytometric analysis. *Cancer* 1994;17:489–503.
46. Tseng SL, Yu IC, Yue CT, Chang SF, Chang TM, Wu CW, et al. Allelic loss at BRCA1, BRCA2 and adjacent loci in relation to TP53 abnormality in breast cancer. *Genes Chromosomes Cancer* 1997;20:377–82.
47. Villeneuve JB, Silverman MB, Alderete B, Cliby WA, Li H, Croghan GA, et al. Loss of markers linked to BRCA1 precedes loss at important cell cycle regulatory genes in epithelial ovarian cancer. *Genes Chromosomes Cancer* 1999;25:65–9.
48. Li C, Larsson C, Futreal A, Lancaster J, Phelan C, Aspenbald U, et al. Identification of two distinct deleted regions on chromosome 13 in prostate cancer. *Oncogene* 1998;16: 481–7.
49. Geck P, Szelei J, Jimmenez J, Sonnenschein C, Soto AM. Early gene expression during androgen-induced inhibition of proliferation of prostate cancer cells: a new suppressor candidate on chromosome 13, in the BRCA2-Rb1 locus. *J Steroid Biochem Mol Biol* 1999;68:41–50.
50. Sobol H, Stoppa-Lyonnet D, Paillerets BB, Peyrat JP, Kerangueven F, Janin N, et al. Truncation at conserved terminal regions of BRCA1 protein is associated with highly proliferating hereditary breast cancers. *Cancer Res* 1996;56: 3216–9.
51. Armes JE, Trute L, White D, Southey MC, Hammet F, Tesoriero A, et al. Distinct molecular pathogenesis of early-onset breast cancers in BRCA1 and BRCA2 mutation carriers: a population-based study. *Cancer Res* 1999;59:2011–7.
52. Suzuki A, Pompa JL, Hakem R, Elia A, Yoshida R, Mo R, et al. Brca2 is required for embryonic cellular proliferation in the mouse. *Genes Dev* 1997;11:1242–52.
53. Serrano M, Lin AW, McCurrach ME, Beach D, Lowe SW. Oncogenic ras provokes premature cell senescence associated with accumulation of p53 and p16INK4a. *Cell* 1997;88: 593–602.
54. Hicks GG, Egan SE, Greenberg AH, Mowat M. Mutant p53 tumor suppressor alleles release ras-induced cell cycle growth arrest. *Mol Cell Biol* 1991;11:1344–52.
55. Damalas A, Ben-Ze'ev A, Simcha I, Shtutman M, Leal JF, Zhurinsky J, et al. Excess beta-catenin promotes accumulation of transcriptionally active p53. *EMBO J* 1999;18:3054–63.
56. Crook T, Brooks LA, Crossland S, Osin P, Barker KT, Waller J, et al. p53 mutation with frequent novel codons but not a mutator phenotype in BRCA1- and BRCA2-associated breast tumours. *Oncogene* 1998;17:1681–9.
57. Smith PD, Crossland S, Parker G, Osin P, Brooks L, Waller J, et al. Novel p53 mutants selected in BRCA-associated tumours, which dissociate transformation suppression from other wild-type p53 functions. *Oncogene* 1999;18:2451–9.
58. Gorgoulis VG, Zacharatos PV, Manolis E, Ikonomopoulos JA, Damalas A, Lamprinopoulos C, et al. Effects of p53 mutants derived from lung carcinomas on the p53-responsive element (p53RE) of the MDM2 gene. *Br J Cancer* 1998;77:374–84.
59. Zacharatos PV, Gorgoulis VG, Kotsinas A, Manolis EN, Liloglou T, Rassidakis AN, et al. Modulation of wild-type p53 activity by mutant p53 R273H depends on the p53 responsive element (p53RE). A comparative study between the p53REs of the MDM2, WAFI/Cip1 and Bax genes in the lung cancer environment. *Anticancer Res* 1999;19:579–87.
60. Jacob AN, Kandpal G, Kandpal RP. Isolation of expressed sequences that include a gene for familial breast cancer (BRCA2) and other novel transcripts from a five megabase region on chromosome 13q12. *Oncogene* 1996;13:213–21.
61. Bieche I, Nogues C, Lidereau R. Overexpression of BRCA2 gene in sporadic breast tumors. *Oncogene* 1999;18: 5232–8.